CDF/PUB/TOP/CDFR/XXXX

Search for Production of an Upsilon(1S) meson in Association with a W or Z Boson in 1.96 TeV $p\bar{p}$ Collisions at CDF

The CDF Collaboration

December 2, 2013

Abstract

The production of the Upsilon(1S) meson in association with a vector boson is a rare process with a standard model cross section predicted to be outside the range of sensitivity at the Tevatron. Observation of this process could signify problems with the current non-relativistic QCD models used for the cross section calculation, or it might signify a contribution from new physics models. We perform a first search for this process using the full $9.7\,\mathrm{fb}^{-1}$ of Run 2 data collected by CDF, using the $\Upsilon \to \mu\mu$ decay together with the charged lepton decay modes of the W and Z bosons. In these purely leptonic decay channels, we observe one $\Upsilon + W$ candidate over an expected background of 1.2 ± 0.5 events, and one $\Upsilon + Z$ candidate over an expected background of 0.1 ± 0.1 events. Having not seen evidence for $\Upsilon + W/Z$ production we calculate cross section limits at 1.96 TeV. These are the best cross section limits for this process, and also provide a guide to limits on new physics processes producing an $\Upsilon + W/Z$.

1 Introduction

The standard model production of an Upsilon meson (Υ) in association with a W boson or a Z boson has been calculated [1] where the ΥW and ΥZ production occur by the parton level processes producing $W + b\bar{b}$ and $Z + b\bar{b}$ final states, where the $b\bar{b}$ pair may form a bound state particle, which can either be an Υ or an excited bottomonium state that decays to an Υ.

The cross sections calculated for ΥW and ΥZ production in proton-antiproton ($p\bar{p}$) collisions at a center-of mass energy of 1.8 TeV (the energy of Run 1 of the Fermilab Tevatron) are 0.45 pb and 0.15 pb, respectively. In Run 2 of the Tevatron, the center-of-mass energy increased to 1.96 TeV where reference [1] expected the cross sections to increase by about 10%. However, the calculations of the processes are very sensitive to the standard model non-relativistic QCD models, especially the numerical values of the long distance matrix elements (LDME), which determine the probability that a $b\bar{b}$ will form a bottomonium state. Therefore, searching for these processes can provide useful input to these non-relativistic QCD models.

Supersymmetry (SUSY) is an extension of the Standard Model, which is yet to be experimentally confirmed. Reference [1] mentions that in some SUSY models, the charged Higgs boson can decay into a Υ+W pair with a large branching ratio. Similarly, the neutral Higgs boson may decay into $\Upsilon + Z$ pair. Therefore, if the observed rate of $\Upsilon + W$ and/or $\Upsilon + Z$ production is significantly larger than the standard model prediction, it may be indicative of the existence of new physics such as these SUSY scenarios.

In 2003, the CDF collaboration published [2] a search for the associated production of an Upsilon meson and a W or a Z boson. In that analysis $83\,\mathrm{pb}^{-1}$ of 1.8 TeV $p\bar{p}$ collision data collected with the CDF detector in Run I of the Tevatron was used.

After a decade, the CDF experiment here presents another search for $\Upsilon + W/Z$

production, using $9700\,\mathrm{pb}^{-1}$ of 1.96 TeV $p\bar{p}$ collision data collected during Run 2 of the Tevatron. We use the dimuon decay channel to identify the Upsilon meson. For the W and Z bosons we use the leptonic decay channels which we found gave us the best sensitivity even though they have smaller branching ratios.

2 The CDF Detector

The CDF II detector is a nearly azimuthally and forward-backward symmetric detector designed to study $p\bar{p}$ collisions at the Tevatron, described in detail in Reference [3]. It consists of a magnetic spectrometer surrounded by calorimeters and muon chambers. Particle positions and angles are expressed in a cylindric coordinate system, with the z axis along the proton beam and the x axis pointing outward from the center of the Tevatron. The azimuthal angle (ϕ) is defined with respect to the x direction. The polar angle (θ) is measured with respect to the z direction, and the pseudo-rapidity (η) is defined as $\eta = -\ln(\tan\frac{\theta}{2})$. The momentum of charged particles is measured by the tracking system, consisting of silicon strip detectors surrounded by an open-cell drift chamber, all immersed in a 1.4 T solenoidal magnetic field. The tracking system provides good tracking efficiency for charged particle out to $|\eta| < 1.0$. The tracking system is surrounded by calorimeters which measure the energies of electrons, photons, and jets of hadronic particles. The electromagnetic calorimeters use a scintillating tile and lead sampling technology, while the hadronic calorimeters are also composed of scintillating tiles with steel absorber. The calorimeters are broken into central and plug sections, with the central region covering the region out to $|\eta| < 1.1$ and the plug extending the coverage to $|\eta| < 3.6$. The muon system is composed of planar multi-wire drift chambers. Four different segments of the muon detector are used for the analysis presented here: the CMU, CMP, CMX, and BMU. In the central region, $|\eta| < 1.5$, four

layers of chambers located just outside of the calorimeter make up the CMU system; the CMU is surrounded by 60 cm of iron shielding and another four layers of chambers compose the CMP system. The CMX covers the region with $0.6 < |\eta| < 1.0$, while the BMU extends the coverage to $|\eta| < 1.5$. Cherenkov Luminosity Counters (CLCs) measure the rate of inelastic collisions, which can be converted to an instantaneous luminosity. The integrated luminosity is calculated from the instantaneous luminosity measurements. The three-level trigger system at CDF is used to reduce the event rate from 1.7 MHz to about 150 Hz. The first level uses hardware, while the second is a mixture of hardware and fast software algorithms. The software based third-level trigger has information very similar to that available online.

3 Monte Carlo and Data Samples

The analysis uses the high-p_T lepton datasets, which have the requirement that the event contain a reconstructed electron or muon with E_T (or p_T in the case of muons) greater than 18 GeV. The integrated luminosity of these samples is $9.7\,\mathrm{fb}^{-1}$. We also use a low-p_T dimuon triggered sample for cross-checks and the estimation of one of the backgrounds. The integrated luminosity of this sample is $7.3\,\mathrm{fb}^{-1}$. The dimuon invariant mass from this sample is shown in Figure 1.

We produce Monte Carlo samples of the signal processes, $\Upsilon + W$ and $\Upsilon + Z$, using MADGRAPH [4] in the CDF Run 2 framework. MADGRAPH allows us to input the latest calculations of the long-range matrix elements (LRME) for Upsilon production. We use the quarkonium extension of MADGRAPH to produce $\Upsilon + W/Z$ events at the generator level. We include all $\Upsilon + W/Z$ processes from Reference [1] and the latest calculated LRMEs from Reference [5], which result in cross section predictions approximately an order of magnitude less than those cited in the former reference due to significant

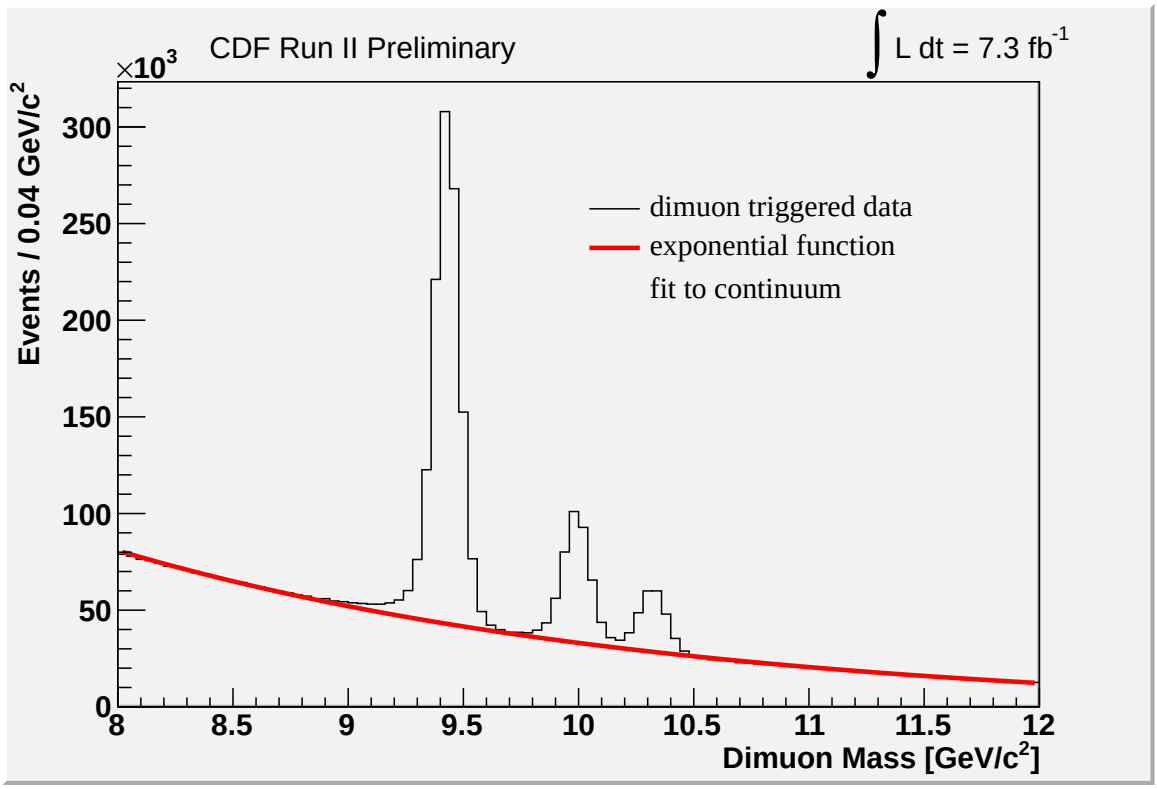

Figure 1: Dimuon invariant mass spectrum in CDF data triggered by two low-P_T muons..

differences in the LRME calculations. We decay $\Upsilon + W/Z$ and shower the events using PYTHIA [6]. At the PYTHIA level, we force the Upsilon to decay to two muons. We simulate the CDF detector using the CDFSIM software package [7].

4 Event Selection

This analysis considers Υ mesons decaying to muon pairs, and decays of the vector bosons that contain at least one charged lepton. The event selection can be divided into three main steps. We first select $\Upsilon(1S)$ candidates using the Υ decay to two low-energy muons. We then look for an additional high-energy lepton (electron or muon) indicative of a vector boson decay. Events with exactly one high-energy lepton (ℓ), in addition to the $\Upsilon \to \mu^+\mu^-$ candidate, and significant missing energy are used to define our $\Upsilon + (W \to \ell\nu)$ candidates. Events with a second oppositely charged high-energy lepton of same flavor are used to define our $\Upsilon + (Z \to \ell^+\ell^-)$ candidates.

Before detailing the selection criteria, we here define some quantities used for event selection. The transverse momentum of a charged particle is $p_T = p \sin\theta$, where p is the momentum of the charged particle track. The analogous quantity measured with calorimeter energies is the transverse energy, $E_T = E \sin\theta$. The missing transverse energy, $\not\!\!E_T$ is defined by $\vec{\not\!\!E}_T = -\sum_i E_T^i \hat{n}_i$, where $\hat{n}_i$ is a unit vector perpendicular to the beam axis and pointing at the i^{th} calorimeter tower. $\vec{\not\!\!E}_T$ is corrected for high-energy muons as well as jet energy corrections. We define $\not\!\!E_T = |\vec{\not\!\!E}_T|$. The invariant mass of two leptons is $M_{\ell\ell} = \sqrt{(E_{\ell 1} + E_{\ell 2})^2 - |\vec{p}_{\ell 1} + \vec{p}_{\ell 2}|^2}$, and the transverse mass of a lepton and neutrino (as measured by the $\not\!\!E_T$) is $M_T = \sqrt{2p_T^\ell \not\!\!E_T (1 - \cos\phi)}$ where ϕ is the angle between the lepton and $\not\!\!E_T$ in the transverse plane.

We define the Upsilon(1S) region as the invariant mass range $9.25 < M_{\mu\mu} < 9.65\,\text{GeV}$. We do not use the Upsilon 2S or 3S states in this analysis. We also de-

fine sideband regions for use in estimating one of our main backgrounds. These are defined by $8.00 < M_{\mu\mu} < 9.00\,\mathrm{GeV}$ and $10.75 < M_{\mu\mu} < 11.75\,\mathrm{GeV}$.

Events are first selected which have at least two low-p_T muons, each of which must satisfy $1.5 < p_T < 15\,\mathrm{GeV}$, and for which the invariant mass of a dimuon pair lies within the Upsilon(1S) region. To increase the Upsilon efficiency we have looser requirements on the low-p_T Upsilon muons than we do for the high-p_T vector boson leptons. In particular, there are no isolation requirements on the Upsilon muons and the matching requirements for the inner track to the muon detector track are not as stringent.

From the above events with a $\Upsilon \to \mu\mu$ candidate we select $\Upsilon + (W \to \ell\nu)$ candidates by requiring exactly one additional electron (muon) with E_T (p_T) greater than 20 GeV. The electron or muon is also required to be isolated from other calorimeter activity: we require that in a cone of $\Delta R = \sqrt{\Delta\eta^2 + \Delta\phi^2} = 0.4$ the additional calorimeter energy to that of the lepton be no more than 10% of the lepton's momentum. We additionally require the event have $\not\!\!E_T > 20\,\mathrm{GeV}$ and that the transverse mass be in the range $50 < M_T < 90\,\mathrm{GeV}$, consistent with that of a W boson. Figure's 2 and 3 show the distributions of these quantities as predicted from the $\Upsilon + W$ signal Monte Carlo samples.

We select $\Upsilon + (Z \to \ell\ell)$ candidates, from events with a $\Upsilon \to \mu\mu$ candidate, by requiring one additional high-p_T electron (muon) with $E_T(p_T) > 20\,\mathrm{GeV}$, and a second lepton of the same flavor and opposite charge with $E_T(p_T) > 15\,\mathrm{GeV}$. Both additional leptons are required to be isolated. To be consistent with both leptons coming from a Z boson decay we require $76 < M_{\ell\ell} < 106\,\mathrm{GeV}$. The invariant mass distributions predicted from $\Upsilon + (Z \to \ell\ell)$ events are shown in Figure 4.

The signal efficiencies, as determined from the Monte Carlo samples, are 1.8% for $\Upsilon + W \to e\nu$, 1.3% for $\Upsilon + W \to \mu\nu$, 1.8% for $\Upsilon + Z \to ee$, and 1.4% for $\Upsilon + Z \to \mu\mu$. These efficiencies do not include the branching ratios of $\Upsilon \to \mu\mu$ and

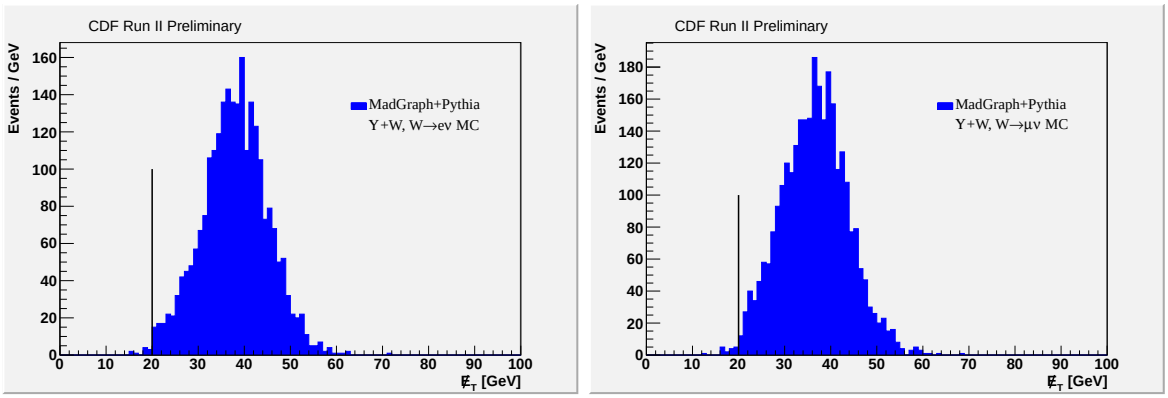

Figure 2: The missing transverse energy spectrums predicted for signal $\Upsilon + W$. The left distribution is for $W \to e\nu$ and the right for $W \to \mu\nu$. The distributions are plotted after all other event requirements are made.

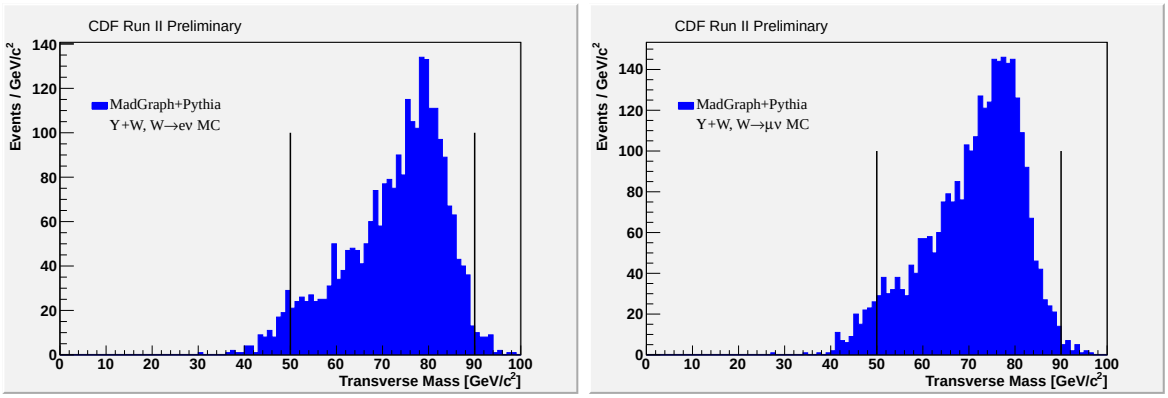

Figure 3: The transverse mass distributions predicted for signal $\Upsilon + W$. The left distribution is for $W \to e\nu$ and the right for $W \to \mu\nu$. The distributions are plotted after all other event requirements are made.

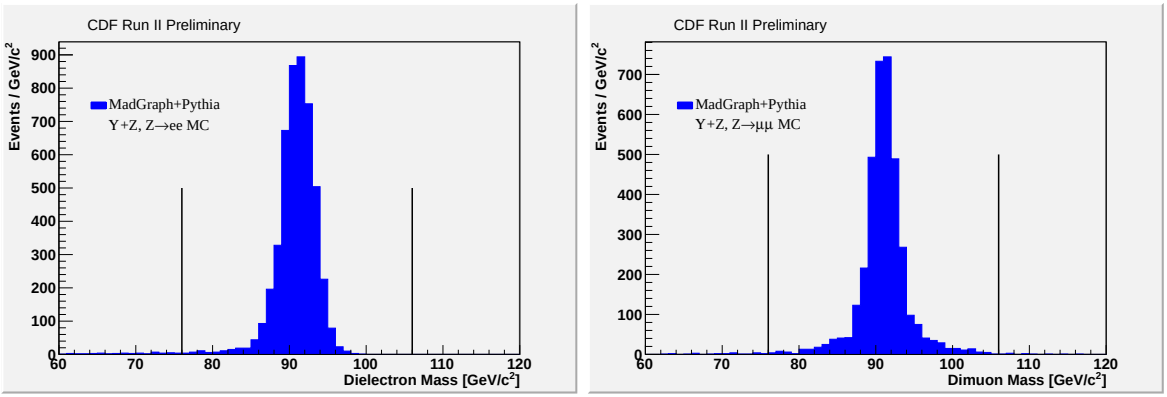

Figure 4: Invariant mass distributions predicted for signal $\Upsilon + Z$ events. The left distribution is the invariant mass of the two additional high-E_T electrons in $\Upsilon + Z$ events, and the right that of the two additional high-p_T muons.

those of the leptonic decays of the vector bosons. The efficiencies are driven by the low detector efficiencies for the low-p_T muons from the Upsilon decay. We expect a small contribution to the $W \to \ell\nu$ acceptance from $W \to \tau\nu$ where the tau lepton decays to an electron or muon. We determined this contribution to be less than 2% of the acceptance, and so it is neglected. The contribution from $Z \to \tau\tau$ to the $Z \to \ell\ell$ channels is negligible.

5 Backgrounds

We have two main backgrounds in this analysis: real W/Z + fake Upsilon, and real Upsilon + fake W/Z. A fake Upsilon can come from the dimuon continuum which is predominantly from $b\bar{b}$. A fake vector boson can come from a jet faking a lepton signature. Due to the small probability for this, the fake Z background is expected to be negligible.

We estimate the fake Upsilon rates using the sideband regions defined above. To estimate the real W/Z + fake Upsilon background, we run the analysis over data, requiring a sideband candidate instead of an Upsilon 1S candidate. The background

in the Upsilon 1S region is estimated by scaling the observed events in the sideband regions by the ratio of their respective areas under an exponential fit.

The fake vector boson rates are estimated using fake lepton probabilities for jets in the event identified as "fakeable", as a function of E_T and the type of lepton that the jet is able to fake, as described in more detail in reference [8]. To estimate real Upsilon + fake W/Z background, we run the analysis over the low-p_T dimuon data sample, requiring high-E_T fakeable jets instead of high-P_T isolated leptons. This data sample is used rather than the high-p_T lepton sample because the fake high-p_T lepton probabilities in the former sample will be unaffected by the trigger requirements. We then apply the appropriate fake probabilities to determine event weights where the total of the event weights gives the background estimates. A correction factor is applied to account for differences in the low-p_T dimuon trigger requirements and the Upsilon muon requirements used in the high-p_T lepton datasets.

The yields from these backgrounds using the methods described are summarized in Table 2. In evaluating the real Z + fake Upsilon contribution, no events were observed in the sideband regions. Therefore, to get an estimate of this background we scaled the real W + fake Upsilon background by the ratio of the Z to W cross sections, under the assumption that the fake Upsilon probability is roughly independent of the vector boson type. In addition, there is a contribution to the $\Upsilon + W$ signal from $\Upsilon + Z$ events where one lepton from the Z decay fails the lepton requirements. Although very small, we include this as a background when calculating the $\Upsilon + W$ cross section limit.

6 Systematic Uncertainties

For the signal expectation, there are systematic uncertainties due to integrated luminosity, Upsilon muon identification, high-P_T lepton identification, high-P_T lepton

trigger efficiency, theoretical modelling of the signal cross section, and event selection efficiencies. The Upsilon muon identification uncertainty is based on previous CDF upsilon measurements [9], while the high-P_T lepton identification and trigger efficiency uncertainties are derived from reference [8].

The default parton distribution functions (PDFs) used in MadGraph is CTEQ6L, which we change to MRST to estimate the PDF uncertainty. We vary the LRMEs by 1 standard deviation to estimate the uncertainty to to the LRMEs, where both the nominal values and their uncertainties are from Reference [5]. In addition, we vary the $\not\!\!E_T$ by $\pm 10\%$ to estimate the event selection efficiency uncertainty. The signal systematic uncertainties are summarized in Table 1.

For the real W/Z + fake Upsilon background, we use the statistical uncertainty which dominates due to very low statistics in the sideband regions used for this estimate. We assign a 50% uncertainty to the real Upsilon + fake W/Z background based on the uncertainties for the fake lepton probabilities.

Luminosity	6%
Upsilon muon ID	4%
High-P_T lepton ID	1%
High-P_T lepton trigger efficiency	1%
PDF	12%
LRME	6%
Event selection efficiency	3%
Total	16%

Table 1: Systematic uncertainties considered for the signal expectation.

7 Results

Table 2 summarizes our signal and background expectations, and the observed events in $9.7\,\mathrm{fb}^{-1}$ of CDF Run 2 data. We observe one $\Upsilon + W \to \ell\nu$ candidate with a total

expected background of 1.2 ± 0.5 events, and one $\Upsilon + Z \to \ell\ell$ candidate with a total expected background of 0.1 ± 0.1 events. An event display of the $\Upsilon + Z \to \ell\ell$ candidate is shown in Figure 5. This is the first $\Upsilon + Z \to \ell\ell$ candidate observed. The two high-p_T muons form an invariant mass of 88.6 GeV, and the two low-p_T muons form an invariant mass of 9.26 GeV. All muons appear in the central region of the detector and are of very good quality. The invariant mass of all four muons is 98.4 GeV.

	$\Upsilon + W \to e\nu$	$\Upsilon + W \to \mu\nu$	$\Upsilon + W \to \ell\nu$	$\Upsilon + Z \to ee$	$\Upsilon + Z \to \mu\mu$	$\Upsilon + Z \to \ell\ell$
N_{sig}	0.019±0.003	0.014±0.002	0.034±0.005	0.0048±0.0007	0.0037±0.0006	0.0084±0.0013
N_{bg} (fake Υ)	0.7±0.4	0.4±0.3	1.1±0.5	0.07±0.07	0.04±0.04	0.1±0.1
N_{bg} (fake W/Z)	0.06±0.04	0	0.06±0.04	0	0	0
N_{bg} ($\Upsilon + Z$)	0.0006±0.0001	0.0033±0.0005	0.0039±0.0006			
N_{bg} (total)	0.8±0.4	0.4±0.3	1.2±0.5	0.07±0.07	0.04±0.04	0.1±0.1
N_{obs}	0	1	1	0	1	1

Table 2: Summary of signal expectation, background estimation and observed events in 9.7 fb^{-1} of 1.96 TeV $p\bar{p}$ collision data at CDF. N_{bg} are the background estimates as described in the text. N_{sig} is the expected signal contribution, and N_{obs} the number of events observed in the data.

Having observed no clear evidence for a $\Upsilon + W/Z$ signal, we set 95% confidence level (CL) limits on the $\Upsilon + W$ and $\Upsilon + Z$ production cross sections (before decay). The limits are obtained using a Bayesian approach with a likelihood function, incorporating all the systematic uncertainties with the appropriate correlations [10]. The expected and observed limits are shown in Table 3 and compared to the observed limits from the CDF Run 1 analysis [2].

	$\Upsilon + W$	$\Upsilon + Z$
expected limit (pb)	5.4	13
observed limit (pb)	5.4	20
Run I observed limit (pb)	93	101

Table 3: Cross section limits at 95% CL. This analysis utilizes 9.4 fb^{-1} of CDF Run 2 data. The Run 1 analysis utilized 83 pb^{-1} of CDF Run 1 data.

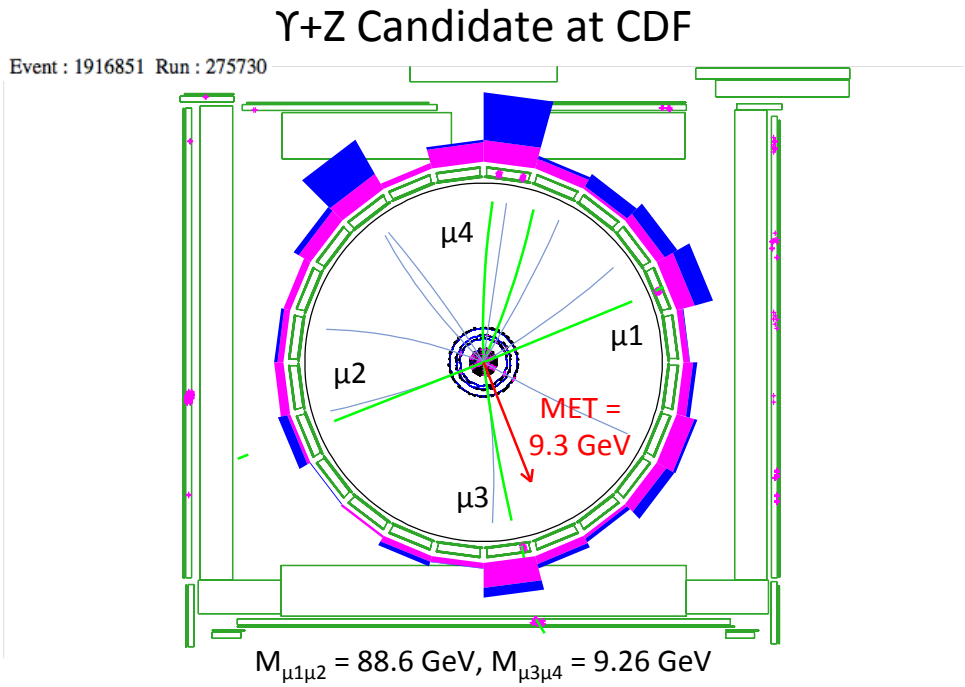

Figure 5: Event display of the observed $\Upsilon + Z$ candidate, showing the muons identified from the Υ and Z decays.

8 Conclusions

We have searched for $\Upsilon + W/Z$ production using the leptonic decay channels of the vector bosons and muonic decay channel of the Upsilon. The search utilizes the full CDF Run 2 dataset. Having observed no significant excess of events we set 95% CL upper limits on the $\Upsilon + W/Z$ cross sections which are the best such limits on these processes. Since it is not expected that new physics contributions to the $\Upsilon + W/Z$ final state will significantly impact the kinematics of the event, these limits also provide an indication of the cross section (times branching ratio to $\Upsilon + W/Z$) limits on any new physics process. New heavy particles decaying to $\Upsilon + W/Z$ will if anything tend to produce leptons that are more central than standard model $\Upsilon + W/Z$ production, hence the limits presented here can be considered as upper limits for such processes.

9 Acknowledgments

We would like to acknowledge K. W. Lai for suggesting the search for these processes, and J.-P. Lansberg for many useful discussions and help with theoretical inputs into the MADGRAPH simulation.

We thank the Fermilab staff and the technical staffs of the participating institutions for their vital contributions. This work was supported by the U.S. Department of Energy and National Science Foundation; the Italian Istituto Nazionale di Fisica Nucleare; the Ministry of Education, Culture, Sports, Science and Technology of Japan; the Natural Sciences and Engineering Research Council of Canada; the National Science Council of the Republic of China; the Swiss National Science Foundation; the A.P. Sloan Foundation; the Bundesministerium fuer Bildung und Forschung, Germany; the Korean Science and Engineering Foundation and the Korean Research Foundation; the Particle Physics and Astronomy Research Council and the Royal Society, UK; the

Russian Foundation for Basic Research; the Comision Interministerial de Ciencia y Tecnologia, Spain; and in part by the European Community's Human Potential Programme under contract HPRN-CT-2002-00292, Probe for New Physics.

References

[1] E. Braaten, J. Lee and S. Fleming, Phys. Rev. D **60**, 91501 (1999).

[2] D. Acosta et al. (CDF Collaboration), Phys. Rev. Lett. **90**, 221803 (2003).

[3] F. Abe et al., Nucl. Instrum. Methods Phys. Res. A **271**, 387 (1988); D. Amidei et al., Nucl. Instum. Methods Phys. Res. A **350**, 73 (1994); F. Abe et al., Phys. Rev. D **52**, 4784 (1995); P. Azzi et al., Nucl. Instrum. Methods Phys. Res. A **360**, 137 (1995); The CDFII Detector Technical Design Report, Fermilab-Pub-96/390-E

[4] J. Alwall, P. Demin, S. de Visscher, R. Frederix, M. Herquet, F. Maltoni, T. Plehn, D. L. Rainwater, and T. Stelzer, J. High Energy Phys. **09** 028 (2007).

[5] E. Braaten, S. Fleming and A. Leibovich, Phys. Rev. D **63**, 094006 (2001).

[6] T. Sjostrand, S. Mrenna, and P. Z. Skands, J. High Energy Phys. **05** 026 (2006).

[7] E. Gerchtein and M. Paulini, eConf **C0303241**, TUMT005 (2003).

[8] T. Aaltonen et al. (CDF Collaboration), Phys. Rev. D **88**, 052012 (2013).

[9] T. Aaltonen et al. (CDF Collaboration), Phys. Rev. Lett. **108**, 151802 (2012).

[10] T. Junk, Sensitivity, exclusion and discovery with small signals, large backgrounds, and large systematics, CDF/DOC/STATISTICS/PUBLIC/8128 (2007).